Journal of Engineering Sciences

Vol 11, Issue 1, JAN/ 2020
ISSN NO:0377-9254

SYNTHESIS OF CHROMIUM OXIDE NANOPARTICLES AT DIFFERENT pH AND THEIR STRUCTURAL AND OPTICAL PROPERTIES

K. Prema Latha[1&2*] and S. Meenakshi Sundar[3]

[1*]Research Scholar (Reg.No. 11639), [2]Assistant Professor, [3]Associate Professor and Head

P.G and Research Department of Physics, Sri Paramakalyani College, Alwarkurichi - 627 412.

Affliated to Manonmaniam Sundaranar University, Abishekapatti, Tirunelveli – 627 012.

**Corresponding Author:* premalathapremi@gmail.com

Abstract

Chromium oxide nanoparticles were synthesized using microwave oven technique for different pH values. Synthesized samples were subjected to XRD and show amorphous. The samples are calcinated at 500 °C for 2 hrs resulted in the formation of chromium oxide nanoparticles. Chromium oxide nanoparticles were characterized by X-ray diffraction (XRD), Fourier transform infrared spectroscopy (FT-IR), UV-Vis spectroscopy, Photoluminescence (PL) and Scanning Electron Microscope (SEM). Cr_2O_3 phase were identified from the XRD data. Debye-scherrer formula was used to calculate the average crystallite size of the prepared nanomaterials and was found to be 25nm to 43 nm. Crystallite size increases with the increase in pH of the solvent (ethylene glycol at varied pH 3, 6, and 10). FT-IR spectrum shows stretching and bending bands at 440, 506, 680 cm^{-1}. UV-Vis spectrum shows the energy band gap < 4 eV. Photoluminescence shows peaks around 400 – 530 nm. The emission is in the visible region. Morphology of the sample was studied by SEM images.

Keywords: *chromium oxide, eskolaite, microwave, debye-scherrer formula, tauc plot*

INTRODUCTION

Inspite of unusual structural geometry, semiconductor metal oxide nanostructures are of great interest of research in nanoscience and nanotechnology, because that this class of compound is frequently revealing the novel properties relative to their coarse-grained counterparts, due to their reduced size and large surface area [1 - 4]. Chromium oxide (Cr_2O_3) occurs in nature as a rare mineral called eskolaite [5]. It is the hardest material and exhibits high hardness values. It is also recognized as a stable oxide in the Cr–O binary system. Other well-known oxides in this system are CrO_3 and CrO_2. This Cr_2O_3 has a wide band gap (Eg ~ 3.4 eV). In recent-past studies [6] many crystalline modifications of chromium oxides: such as rutile (CrO_2), CrO_3, CrO_4, corundum (Cr_2O_3), Cr_2O_5, and Cr_5O_{12} has been reported. Among these modifications, Cr_2O_3 is the most stable magnetic-dielectric oxide-material [7]. The synthesis and formation of Cr_2O_3 have been focused with special attention among the other metal oxides because these nanomaterials are predominantly used as a dye, heterogeneous catalyst [8], coating material, wear resistance [9], advanced colorant [10], pigment [11] and solar energy collector [12].

Various techniques for the synthesis of Cr_2O_3 nanoparticles such as hydrothermal [13], sol-gel [14], combustion [15], precipitation-gelation, gel citrate [16], mechanochemical process [17], urea assisted homogeneous precipitation [18,19], gas condensation [20], and microwave plasma have been developed [21]. Here in the present study, we report the microwave synthesis of chromium oxide, along with its structural and optical properties.

MATERIALS

Analar grade chromium (III) chloride (hexahydrated), urea, ethylene glycol, HCl, NaOH and acetone were purchased from HPLC, India. De-ionized water was used throughout the experiment.

SYNTHESIS

Chromium oxide nano particles were synthesised in the following method. Chromium (III) chloride and urea were taken in 1:3 molecular ratio, mixed and dissolved in 50 ml of ethylene glycol using a magnetic stirrer. Samples were stirred at room temperature for 1hr and kept aside for an hour, for residues (if any) to settle down. The clear transparent solution was transferred to a ceramic bowl. The solution was placed in a domestic microwave oven; due to microwave heating solvents get evaporated completely. A precipitate was formed at the bottom of the bowl. These precipitates were carefully collected and washed with deionized water for several times to remove the ions possibly remaining in the final products, and then washed with acetone for several times to remove the unwanted organic compounds, if any. Three samples of different pH were taken for this study by changing the pH of the ethylene glycol. The pH of ethylene glycol was kept as such for sample B (pH 6) and for other samples pH of ethylene glycol was made to 10 (sample C) and 3 (sample A).

Ethylene glycol was used as a solvent as well as capping agent. The pH value of 50 ml ethylene glycol solvent was increased by adding NaOH solution. For increasing the pH, 0.1 N NaOH solution was prepared and added in drops to ethylene glycol. To decrease the pH of ethylene glycol, 4N HCl solution was prepared and diluted HCl was added in drops to ethylene glycol to reach the desired pH.

In this paper, we report the synthesis and characterization of the chromium oxide with the effect of change in the pH of the solvent. The crystal structures were characterized by x-ray diffraction (XRD) analysis. Morphological structures were observed by scanning electron microscopy (SEM). The functional groups present in the samples were identified by fourier transform infrared spectroscopy (FTIR). The optical studies were carried out using UV-Vis and photoluminescence studies.

RESULT AND DISCUSSION

STRUCTURAL CHARACTERIZATION

XRD

X-ray diffraction (XRD) spectra of samples were recorded in a PANalytical Model X'pert pro X-ray diffractometer employing CuKα radiation at 40 kV and 100 mA at a scanning rate of 8^o min^{-1} in the range 10-80^o. The prepared samples were amorphous in nature hence the samples were calcinated at 500°C for 2 hrs. XRD pattern of annealed Cr_2O_3 nanoparticles (sample A) is shown in fig. 1. XRD shows sharp and intense peaks which confirm the formation of Cr_2O_3 nanoparticles which are crystalline in nature and has single phase. The various angular positions are at 24.55°, 33.58°, 36.20°, 41.46°, 50.17°, 54.84°, 63.38°, 65.10° and 72.99° which are indexed to the plane (012), (104), (110), (113), (024), (116), (214), (300) and (1 0 10) respectively. These peak positions matches well with JCPDS file number; 38-1479. This is in line with the pure eskolaite phase of green Cr_2O_3 [22]. The obtained values of d-spacing are in good agreement with the reported values and thus confirming the rhombo-centered rhombohedral structure of the annealed sample and it belongs to R-3c space group. The lattice constant of Cr_2O_3 nanostructures is a = b = 4.9614 Å & c = 13.5849 Å. Cell volume is 289.596 $Å^3$. The particle size along high intense peak (116) was found to be 25.98 nm.

Lattice constant of a hexagonal structure were evaluated using equation (1) [23]

$$1/d^2 = 4/3\ \{(h^2+ kh +k^2)/a^2\} + (l^2/c^2) \quad \text{---------- (1)}$$

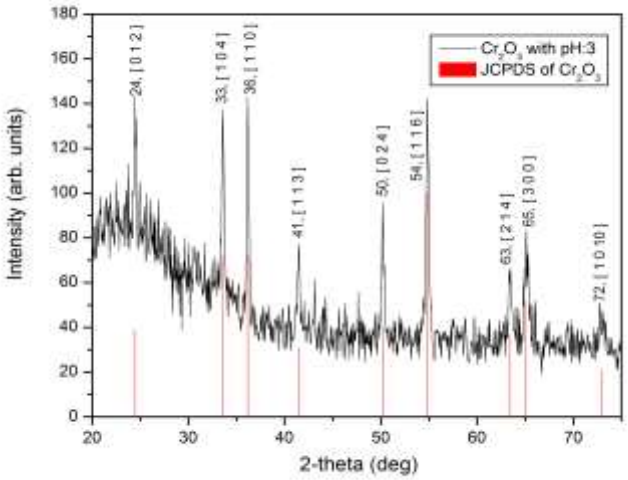

Fig. 1: XRD pattern of Cr_2O_3 (sample-A) nanoparticle

XRD pattern of Cr_2O_3 nanoparticles (Sample B) is shown in fig. 2. XRD shows intense peaks at various angular positions at 24.59°, 33.68°, 36.31°, 41.59°, 50.33°, 54.91°, 58.57°, 63.52°, 65.21°, 73.01° and 77.08° which are indexed to the plane (012), (104), (110), (113), (024), (116), (122), (214), (300), (1 0 10) and (220) respectively. These peak positions matches well with JCPDS file number; 84-1616. This agrees with the pure eskolaite phase of green Cr_2O_3 [24]. The obtained values of d-spacing are in good agreement with the reported values and thus confirming the rhombohedral structure of the annealed sample with pH of the solvent, ethylene glycol, is in Cr_2O_3 nanostructures. The lattice constant of Cr_2O_3 nanostructures is a = b = 4.9474 Å & c = 13.5826 Å. Cell volume is 287.92 $Å^3$. The particle size of the intense peak (104) was found to be 33.73 nm

.

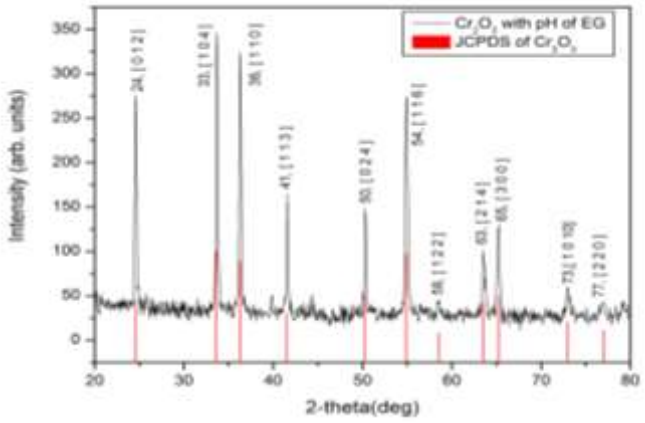

Fig. 2: XRD pattern of Cr_2O_3 (sample-B) nanoparticle

XRD pattern of Cr_2O_3 (sample-c) nanoparticles is shown in fig. 3. The XRD shows intense peaks at the various angular positions at 24.57°, 33.67°, 36.29°, 39.79°, 41.56°,50.29°, 54.90°, 63.49°, 65.17°, 72.95° and 76.95° which are indexed to the plane (012), (104), (110), (006), (113), (024), (116), (214), (300), (1 0 10) and (220) respectively. These peak positions matches well with JCPDS file number; 74- 0326 [25]. This belongs to pure Eskolaite phase of green α-Cr_2O_3. The value of d-spacing confirms the rhombo centered rhombohedral structure with space group R-3c is in α-Cr_2O_3

nanostructures. The lattice constant of α-Cr_2O_3 nanostructures is a = b = 4.9516 Å & c = 13.5836 Å. Cell volume is 288.42 $Å^3$. The average particle size for the intense peak (110) was found to be 42.47 nm.

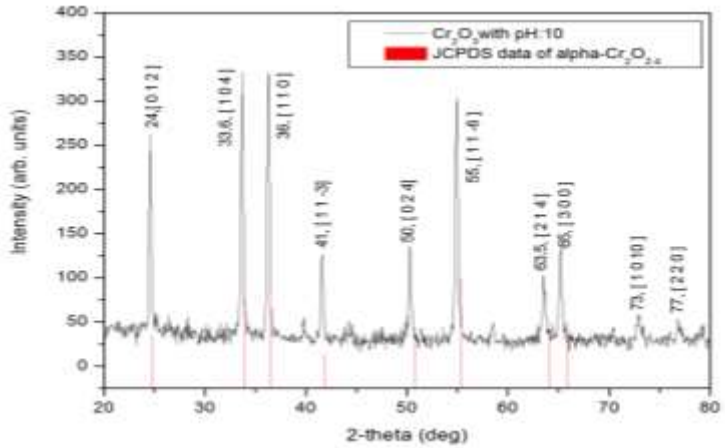

Fig. 3: XRD pattern of α-Cr_2O_3 nanoparticles

The lattice parameter of a rhombohedral structure was calculated from [23]

$$a_R = 1/3\ \sqrt{(3*a_H^2 + c^2)};$$
$$\sin(\alpha/2) = 3/(2*\sqrt{(3 + (c/a_H)^2)} \text{ and}$$
$$V_R = a_R^3 * \sqrt{(1 - 3\cos^2\alpha + 2\cos^3\alpha)} \quad \text{(2)}$$

where, a_R is the lattice parameter of rhombohedral structure; a_H and c are the lattice parameter of hexagonal structure; α is the lattice angle of rhombohedral structure; V_R is the volume of rhombohedral strucuture. The lattice parameters of the three samples are given in table.1

Table. 1: Lattice parameter of the synthesised samples

Sample	Hexagonal structure			c/a ratio	Rhombohedral Structure			Ref
	Lattice Parameter		Cell volume		Lattice Parameter		Cell volume	
	a (Å)	c (Å)			a (Å)	α (°)		
A (pH 3)	4.9614	13.5849	289.59	2.738	5.3582	55.1578	96.53	Farzaneh [26] a = 4.9752 Å and c = 13.8178 Å.
B (pH 6)	4.9474	13.5826	287.92	2.745	5.3532	55.0443	95.97	
C (pH 10)	4.9516	13.5837	288.42	2.743	5.3548	55.0771	96.14	

Table. 2: Particle size of the high intense XRD peak

Sample	2θ With rel.int 100% (deg)	FWHM	d-spacing	h, k, l	D (nm)
A (pH 3)	54.8452	0.3444	1.6739	1,1,6	25.98
B (pH 6)	33.6896	0.2460	2.6604	1,0,4	33.73
C (pH 10)	36.2974	0.1968	2.4750	1,1,0	42.47

The observed value of c/a = 2.738 for sample A and 2.74 for samples B & C, it matches with the standard value of 2.742 of the bulk rhombohedral structure. When compared with the bulk value, the obtained value is slightly less. This gives clear evidence for the existence of compressive strains in the nanopowders as mentioned by Sone et al [24].

From table. 2, the crystallite size of the nanomaterial increases with the increase in the pH value. When the pH is 3 the crystallite size (D) of the material is 25.98 nm. When the solvent pH decreases, crystallite size of the material also decreases. When NaOH is added to solvent, crystallite size increases and in other hand, when acid nature of the solvent increases, crystallite size decreases. The pH concentration versus the crystallite size was given in fig. 4

.

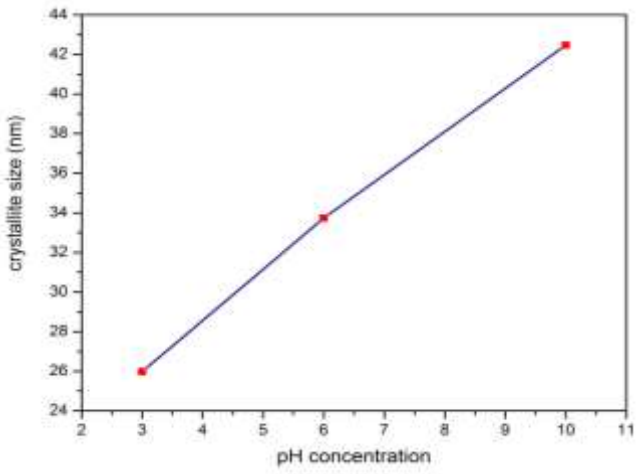

Fig. 4 pH concentration vs crystallite size for Cr_2O_3 nanoparticle

FTIR:

FTIR spectrum of Cr_2O_3 NPs is shown in fig. 5. Chromium oxide nanoparticles generally have their absorption bands below 1000 cm^{-1} (as the metal oxides reveal absorption bands below 1000 cm^{-1}) due to inter-atomic vibrations. The two sharp peaks at 608 and 533 cm^{-1} are due to M-O (Cr-O) stretching modes, which gives a clear evidence for the presence of crystalline Cr_2O_3 [27]. FTIR Spectrum shows two peaks at 533 and 608 cm^{-1} due to M-O (Cr-O) stretching and a sharp peak at 440 cm^{-1} [26].

The vibrational band at 554-564 cm^{-1} characterizes Cr-O distortion vibration, and the bands at 608 and 535 cm^{-1} identify the chromium oxide is in Cr_2O_3 phase. The vibrational modes observed at 440, 506, 535, 608 cm^{-1} are typically of metal oxide single bonds in bending and stretching modes. The relatively weak absorption band at 440 cm^{-1} and the strong broad absorption band at 506 and 535 cm^{-1} can be attributed to Cr-O bonds in the bending mode. While the absoption band at 608 cm^{-1} is due to the Cr-O stretching vibration mode gives a clear evidence for the presence of crystalline α-Cr_2O_3 as stated by Salah A. Makhloaf et al [28].

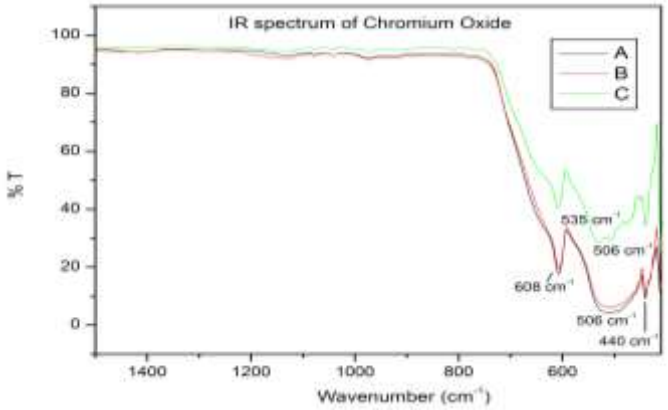

Fig. 5: FTIR spectra of Cr_2O_3 nanoparticle

Table. 3: Functional group of Chromium oxide nanoparticle

Sample	M-O (Cr-O) stretching cm^{-1}		Ref
A (pH 3)	608	506	Farzaneh [26] 652 cm^{-1}, 562 cm^{-1} Gibot [29] 613 cm^{-1}, 541 cm^{-1}
B (pH 6)	608	506	
C (pH 10)	608	535	

OPTICAL PROPERTIES:

UV- Vis

The optical absorption peaks for Cr_2O_3 nanoparticles are seen along 360.16, 354.86 and 346.92 nm for the samples A, B and C respectively. As the crystallite size of the nanomaterial decreases, the peaks of the material appear to be broader. The UV-Vis spectrum for the samples A, B and C is shown in fig. 6.

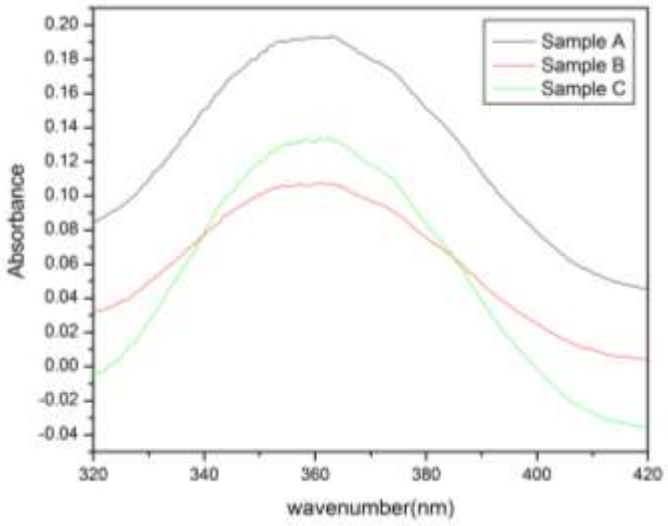

Fig. 6: UV absorption spectra of samples A, B and C

As crystallite size of nanomaterial increases, there is a blue shift in the peaks of absorption spectra, when moving from the samples A to C. The energy band gap of the nanomaterial is calculated using the tauc plot. Crystallite size, optical absorption peak and its energy band gap are tabulated in table. 4.

Table. 4: Energy band gap of samples A, B and C

Sample	Crystallite size, D (nm)	Optical absorption peak (nm)	Eg (eV)	Ref
A (pH 3)	25.98	360.16	3.44	K. Anandhan [30]
B (pH 6)	33.73	354.86	3.5	
C (pH 10)	42.47	346.92	3.58	

The energy band gap of these Cr_2O_3 nanoparticles is estimated using the Tauc relation [6].

$$\alpha h\upsilon = A(h\upsilon - Eg)^n \quad \text{---------- (3)}$$

where α is absorption coefficient, hυ is the photon energy, Eg is the band gap n=1/2 for the direct transitions [31, 6]. A plot of $(\alpha h\upsilon)^2$ versus hυ is shown in fig. 5.7 (a - c) and linear portion of curve is extrapolated to hυ axis to determine band gap. Band gap energy of samples A, B and C are given in table. 4.

Energy band gap of sample A is 3.44 eV, sample B is 3.5 eV and Sample C is 3.58 eV. Absorbance peak is red shifted from A to C. Energy band gap of the α-Cr_2O_3 nanostructures has been determined to be 3.44 eV to 3.58 eV, which confirms Cr_2O_3 nanomaterial has semiconducting property. The tauc plot for the samples A, B and C are given in the Fig. 7 (a - c) respectively.

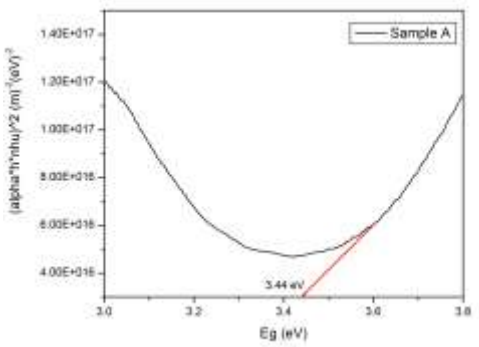

(a)

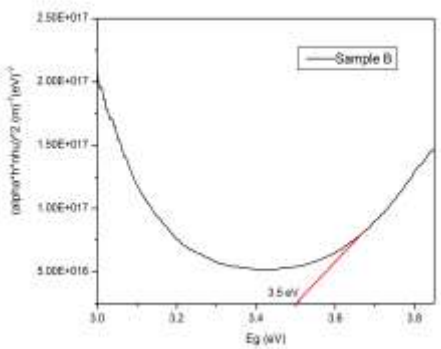

(b)

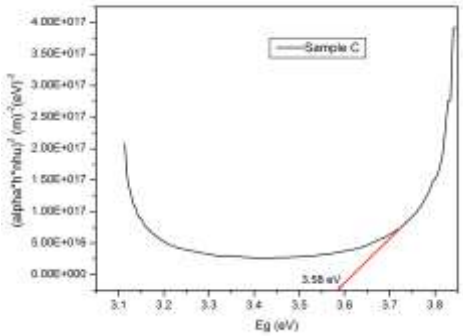

(c)

Fig. 7 (a-c): UV-VIS spectra of Cr_2O_3 nanoparticle

PHOTOLUMINESCENCE

The PL spectra of Cr_2O_3 nanoparticles for samples A, B and C are shown in fig. 8. The spectra show a sharp intense peak at 407 nm for all samples A, B and C. The spectra shows emission peaks at 407, 418, 490 and 518 nm for all the samples which matches with the bulk and nanomaterial value as reported by Farzaneh [26].

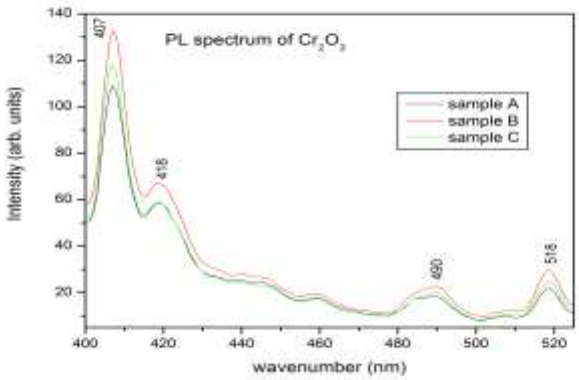

Fig. 8: PL spectra of Cr_2O_3 nanoparticle

SEM

SEM micrograph of Cr_2O_3 calcinated at 500 °C is shown in fig. 9 (a – b are SEM images of sample – A; c – d are SEM images of sample – B; e - g are SEM images of sample - C). It can be seen that the particles for all samples are spherical in morphology and are evenly sized, and particles are agglomerated at the surface. Spherical shaped formations were aggregated in the form of clusters.

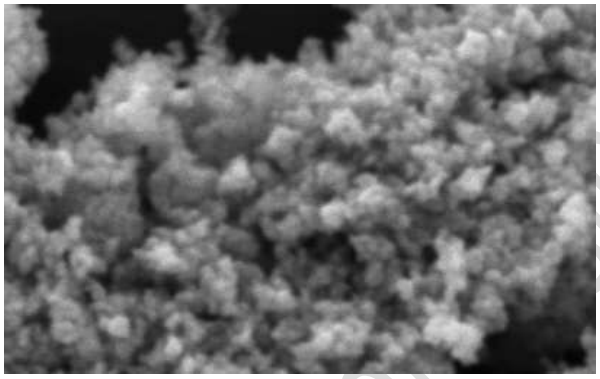

(a)

(b)

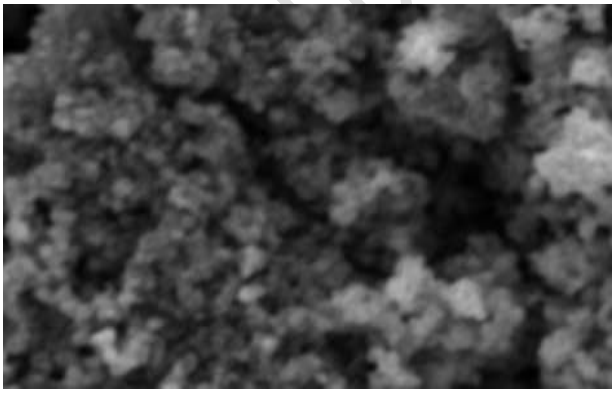

(c)

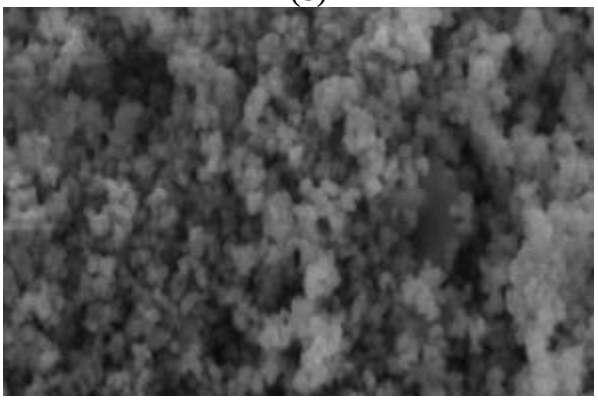

(d)

(e)

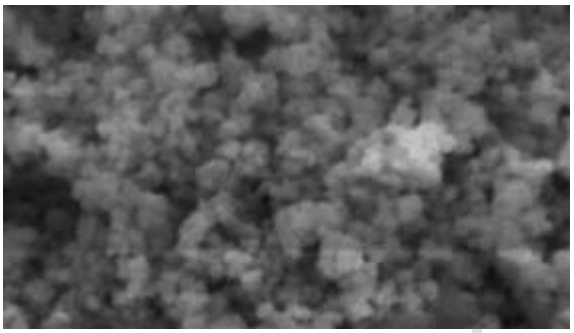

(f)

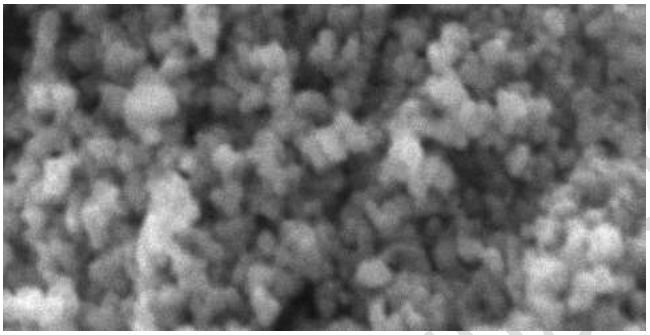

(g)

fig. 9 (a-g): SEM images of Chromium oxide

CONCLUSION

Chromium oxide nanocrystals were synthesized using microwave oven technique with three different pH values. XRD confirms that, the synthesized nanomaterials have Cr_2O_3 phase with rhombo centered rhombohedral structure for all the samples. Particle size of synthesized nanomaterials, increases with the increase in pH concentration. SEM micrograph of Cr_2O_3 calcinated at 500 °C reveals that the particles are spherical in morphology and are evenly sized.

Acknowledgement

One of the author, K. Prema Latha, thanks the UGC-SERO, Hyderabad, India, for awarding the teacher fellowship under Faculty Development Programme vide F.No. FIP-TNMS039/003(TF)/ PHYSICS/Ph.D/XII PLAN/2015-16 dated 20 october 2015.

REFERENCE

[1] Faisal, M, Khan, SB, Rahman, MM, Jamal, A, Asiri, AM & Abdullah, MM 2011, 'Smart chemical sensor and active photo-catalyst for environmental pollutants' Chemical Engineering Journal, vol. 173, no. 1, pp. 178-184. doi:10.1016/j.cej.2011.07.067.

[2] Balouria, V, Singh, A, Debnath, AK, Mahajan, A, Bedi, RK, Aswal, DK & Gupta, SK 2012, 'Synthesis and characterization of sol-gel derived Cr_2O_3 nanoparticles'. AIP Conf. Proc., vol. 1447, no. 1, pp. 341. doi:10.1063/1.4710019.

[3] Abdullah, MM, Rajab, FM & Al-Abbas, SM 2014, 'Structural and optical characterization of Cr2O3 nanostructures: Evaluation of its dielectric properties', AIP ADVANCES, vol. 4, no. 2, pp. 027121.

[4] Blessy Babukutty, Fasalurahman Parakkal, Bhalero, GM, Aravind, PB & Swapna SN 2015, 'Structural, morphological and optical properties of chromium oxide nanoparticles', AIP Conference Proceedings, vol. 1665, no. 1, pp. 050148; doi: 10.1063/1.4917789.

[5] Dymshits, AM, Dorogokupets, P I, Sharygin, IS, Litasov, KD, Shatskiy, A,

Rashchenko, SV, & Higo, Y 2016, 'Thermoelastic properties of chromium oxide Cr2O3 (eskolaite) at high pressures and temperatures', Physics and Chemistry of Minerals, 43(6), 447–458. doi:10.1007/s00269-016-0808-7.

[6] Ivanova, T, Gesheva, K, Cziraki, A, Szekeres, A & Vlaikova, E 2008, 'Structural transformations and their relation to the optoelectronic properties of chromium oxide thin films', Journal of Physics: Conference Series, vol. 113, pp. 012030.

[7] Feng Gu, Chunzhong Li, Yanjie Hu & Ling Zhang 2007, 'Synthesis and optical characterization of Co3O4 nanocrystals', J. Cryst. Growth, vol. 304, no. 2, pp. 369-373.

[8] Rao, TVM, Yang, Y & Sayari, A 2009, 'Ethane dehydrogenation over pore-expanded mesoporous silica supported chromium oxide: 1.Catalysts preparation and characterization', J. Mol. Catal. A: Chem., vol. 301, pp. 152-158.

[9] Pang, X, Gao, K, Luo, F, Emirov, Y, Levin, AA & Volinsky, AA 2009, 'Investigation of micro structure and mechanical properties of multi-layer Cr/Cr2O3 coatings', Thin Solid Films, vol. 517, pp. 1922–1927.

[10] Kim, DW, Shin, SI, Lee, JD & Oh, SG 2004, 'Preparation of chromia nanoparticles by precipitation–gelation reaction', Mater. Lett., vol. 58, pp. 1894-1898.

[11] Li, P, Xu, HB, Zhang, Y, Li, ZH, Zheng, SL & Bai, YL 2009, 'The effects of Al and Ba on the colour performance of chromic oxide green pigment', Dyes and Pigments, vol. 80, pp. 287-291.

[12] Teixeira, V, Sousa, E, Costa, MF, Nunes, C, Rosa, L, Carvalho, MJ, Collares-Pereira, M, Roman, E & Gago, J 2001, 'Spectrally selective composite coatings of Cr-Cr_2O_3 and Mo-Al2O for solar energy applications', Thin Solid Films, vol. 392, pp. 320-326.

[13] Pei, Z, Xu, H & Zhang, Y 2009, 'Preparation of Cr_2O_3 nanoparticles via C_2H_5OH hydrothermal reduction' Journal of Alloys and Compounds, vol. 468, no. 1-2, pp. L5-L8. doi:10.1016/j.jallcom.2007.12.086.

[14] El-Sheikh, SM, Mohamed, RM & Fouad, OA 2009, 'Synthesis and structure screening of nanostructured chromium oxide powders', J. Alloys Compd, vol. 482, pp. 302-307.

[15] Fu, XZ, Luo, XX, Luo, JL, Chuang, KT, Sanger, AR & Krzywicki, A 2011, 'Ethane dehydrogenation over nano- Cr_2O_3 anode catalyst in proton ceramic fuel cell reactors to co-produce ethylene and electricity', J. Power Sources, vol. 196, pp. 1036-1041.

[16] Kim, DW & Oh, SG 2005, 'Agglomeration behaviour of chromia nanoparticles prepared by amorphous complex method using chelating effect of citric acid', Mater. Lett., vol. 59, pp. 976-980.

[17] Li, L, Yan, Z, Lu, GQ & Zhu, ZH 2006, 'Synthesis and structure characterization of chromium oxide prepared by solid thermal decomposition reaction', J. Phys. Chem. B, vol. 110, pp. 178-183.

[18] Abecassis-Wolfovich, M, Rotter, H, Landau, MV, Korin, E, Erenburg, AI, Mogilyansky, D & Gartstein, E 2003, 'Texture and nanostructure of chromia aerogels prepared by urea-assisted homogeneous precipitation and low temperature super critical drying' J. Non-Cryst. Solids, vol. 318, pp. 95-111.

[19] Ocana, M 2001, 'Nanosized Cr_2O_3 hydrate spherical particles prepared by urea method', J. Eur. Ceram. Soc., vol. 21, pp. 931-939.

[20] Balchandran, U, Siegel, RW, Liao, YX & Askew, TR 1995, 'Synthesis, sintering and magnetic properties of nanophase Cr_2O_3', Nanostruct. Mater., vol. 5, pp. 505-512.

[21] Vollath, D, Szabo, DV & Willis, JO 1996, 'Magnetic properties of nanocrystalline Cr_2O_3 synthesized in a microwave plasma', Mater. Lett., vol. 29, pp. 271-279.

[22] Aghaie-Khafri, M & Kakaei Lafdani, MH 2012, 'A novel method to synthesize Cr_2O_3 nanopowders using EDTA as a chelating

agent', Powder Technology, vol. 222, pp. 152-159.

[23] Cullity, BD 1978, 'Elements of X-ray diffraction', 2nd edition, Addison-Wesley Publishing Company Inc.

[24] Sone, BT, Manikandan, E, Gurib-Fakim, A & Maaza, M 2016, 'Single-phase α-Cr_2O_3 nanoparticles' green synthesis using *Callistemon viminalis*' red flower extract', Green Chemistry Letters And Reviews, vol. 9, no. 2, pp. 85-90. doi: 10.1080/17518253.2016.1151083

[25] Khamlich, S, Nemraoui, O, Mongwaketsi, N, McCrind, R, Cingo, N, & Maaza, M 2011, 'Black Cr/a-Cr2O3 nanoparticles based solar absorbers', Physica B. doi:10.1016/j.physb.2011.09.073.

[26] Farzaneh, F & Najafi, M 2011, 'Synthesis and characterization of Cr_2O_3 nanoparticles with triethanolamine in water under microwave irradiation', Journal of Sciences, Islamic Republic of Iran, vol. 22, no. 4, pp. 329-333.

[27] Henderson, MA 2010, 'Photochemistry of methyl bromide on the α-Cr_2O_3 (0001) surface', Surf. Sci, vol. 604, no. 19-20, pp. 1800-1807.

[28] Makhlouf, SA, Bakr, ZH, Al-Attar, H & Moustafa, MS 2013, 'Structural, morphological and electrical properties of Cr_2O_3 nanoparticles', Materials Science and Engineering B, vol. 178, pp. 337-343.

[29] Gibot, P & Vidal, L 2010, 'Original synthesis of chromium (III) oxide nanoparticles', Journal of the European Ceramic Society, vol. 30, pp. 911-915.

[30] Anandan, K & Rajendran, V 2014, 'Studies on structural, morphological, magnetic and optical properties of chromium sesquioxide (Cr_2O_3) nanoparticles: Synthesized via facile solvo thermal process by different solvents', Materials Science in Semiconductor Processing, vol. 19, pp. 136-144.

[31] Abdullah, MM, Preeti Singh, Hasmuddin, M, Bhagavannarayana, G & Wahab, MA 2013, 'In-situ growth and ab-initio optical characterizations of amorphous Ga_3Se_4 Thin Film: A new chalcogenide compound semiconductor thin film', Scripta Materialia, vol. 69, pp. 381.